Stable desensitization of α_7 nicotinic acetylcholine receptors by NS6740 requires interaction with S36 in the orthosteric agonist binding site

Maria Chiara Pismataro [a, b, 1], Nicole A. Horenstein [b], Clare Stokes [c], Clelia Dallanoce [a, *], Ganesh A. Thakur [d], Roger L. Papke [c]

[a] *Department of Pharmaceutical Sciences, Medicinal Chemistry Section "Pietro Pratesi", University of Milan, Via L. Mangiagalli 25, 20133 Milan, Italy*

[b] *Department of Chemistry, University of Florida, P.O. Box 117200, Gainesville, FL 32611-7200, USA*

[c] *Department of Pharmacology and Therapeutics, University of Florida, P.O. Box 100267, Gainesville, FL 32610-0267, USA*

[d] *Department of Pharmaceutical Sciences, School of Pharmacy, Bouvé College of Health Sciences, Northeastern University, Boston, MA 02115*

---

* Corresponding author.

E-mail address: clelia.dallanoce@unimi.it (C. Dallanoce)

[1] Present address: Department of Pharmaceutical Sciences, University of Perugia, Via del Liceo 1, 06123 Perugia, Italy

ABSTRACT

NS6740 is an α_7 nicotinic acetylcholine receptor-selective partial agonist with low efficacy for channel activation, capable of promoting the stable conversion of the receptors to nonconducting (desensitized) states that can be reactivated with the application of positive allosteric modulators (PAMs). In spite of its low efficacy for channel activation, NS6740 is an effective activator of the cholinergic anti-inflammatory pathway. We observed that the concentration-response relationships for channel activation, both when applied alone and when co-applied with the PAM PNU-120596 are inverted-U shaped with inhibitory/desensitizing activities dominant at high concentrations. We evaluated the potential importance of recently identified binding sites for allosteric activators and tested the hypotheses that the stable desensitization produced by NS6740 may be due to binding to these sites. Our experiments were guided by molecular modeling of NS6740 binding to both the allosteric and orthosteric activation sites on the receptor. Our results indicate that with α_7C190A mutants, which have compromised orthosteric activation sites, NS6740 may work at the allosteric activation sites to promote transient PAM-dependent currents but not the stable desensitization seen with wild-type α_7 receptors. Modeling NS6740 in the orthosteric binding sites identified S36 as an important residue for NS6740 binding and predicted that an S36V mutation would limit NS6740 activity. The efficacy of NS6740 for α_7S36V receptors was reduced to zero, and applications of the compound to α_7S36V receptors failed to induce the desensitization observed with wild-type receptors. The results indicate that the unique properties of NS6740 are due primarily to binding at the sites for orthosteric agonists.

Keywords:

α_7 nicotinic acetylcholine receptor

Silent agonist

Partial agonist

Allosteric activation

Docking analysis

Site-directed mutant

1. Introduction

The α_7-type nicotinic acetylcholine receptor has unique biophysical properties, including rapid desensitization and high fractional calcium permeability (Castro and Albuquerque, 1995; Fucile et al., 2003; Seguela et al., 1993) of acetylcholine-evoked responses. Even though the ion channel currents activated by acetylcholine and choline are small and diminish rapidly due to receptor desensitization (Papke, 2014), α_7 receptors are sensitive to various positive allosteric modulators (PAMs) (Williams et al., 2011a), some of which will destabilize desensitized states, generating large current responses.

The α_7 mediated calcium signaling can contribute to synaptic development and functional plasticity through calpain protease activation (King and Kabbani, 2018) and has been implicated in the pathology of neurodevelopmental and neurodegenerative diseases. The α_7 receptor is thus a therapeutic target for a variety of cognitive disorders (Cannon et al., 2013; Kong, et al., 2015; Pieschl et al., 2017; Timmermann et al., 2012; Wallace, et al., 2011), including Schizophrenia and Alzheimer's disease (AD). In particular, in the latter, a specific binding of oligomeric amyloid β peptide to α_7 has been demonstrated, and compounds able to disrupt this interaction represent promising AD therapeutic candidates (Cecon et al., 2019). Moreover, although all the nicotinic subtypes have roles in regulating dopamine-mediated neurotransmission in the mesolimbic reward pathways for reducing or stopping smoking (Jordan and Xi, 2018), unique are the roles of the α_7 in behavioral responses to nicotine, and its activity manipulation appears to be a promising target for smoking relapse prevention (Papke et al., 2020a). The α_7 inhibition may in addition contribute to the effect of antidepressant drugs that block nicotinic currents and calcium signals (Nanclares et al., 2018).

Targeting the α_7 nicotinic acetylcholine receptor is also of therapeutic importance for pain and inflammatory disease (Bagdas et al, 2018; El Nebrisi et al., 2018; Di Cesare Mannelli et al., 2014). The α_7 activation attenuates the production of proinflammatory cytokines and inhibits the inflammatory process through the cholinergic anti-inflammatory pathway (de Jonge and Ulloa, 2007). Different mechanisms are involved in the α_7 anti-inflammatory effects. Acetylcholine and the α_7 partial agonist GTS-21 prevent macrophage activation and suppress inflammation by inhibiting extracellular high mobility group box 1 protein (HMGB1), which binds other immune-activating molecules that are endocytosed via the receptor for advanced glycation end-products (RAGE) (Yang et al., 2019). The anti-colitic anti-inflammatory effects of the reversible competitive acetylcholinesterase inhibitor Galantamine originates from the stimulation of the peripheral nicotinic α_7 receptor with the involvement of the nuclear factor kappa B (NF-κB)/HMGB1/RAGE signaling pathway and the Janus kinase (JAK)/signal transducer and activator of transcription3 (STAT3) cascade (Wazea et al., 2018). Recently, α_7 anti-inflammatory effects are also found to be dependent on adenylyl cyclase 6 activation, which promotes degradation of Toll-like Receptor 4 (TLR4) belonging to the TLR family that induces pro-inflammatory responses (Zhu et al., 2021).

The α_7 receptor plays a crucial role in inflammation control in numerous pathophysiological conditions, including acute and chronic diseases such as obesity (Qi et al., 2020; Scabia et al., 2020) and atherosclerosis (Ulleryd et al., 2019). However, growing interest in α_7 as a therapeutic target for treating inflammation came from studies showing that α_7 expression in non-neuronal cells, i.e. immune system, mediates a specific cholinergic anti-inflammatory pathway (Rosas-Ballina and Tracey, 2009), acting more as a metabotropic receptor than as a ligand-gated ion channel (Kabbani and Nichols, 2018). The pharmacology of α_7 receptors in the cholinergic anti-

inflammatory pathway is different from the pharmacology for channel activation, and some of the best candidate drugs have such low efficacy for channel activation that they have been classified as "silent agonists" (Horenstein and Papke, 2017). Drugs identified as silent agonists regulate the conformational dynamics of the receptor because they effectively induce desensitized states that can be destabilized by type II PAMs such as 1-(5-chloro-2,4-dimethoxyphenyl)-3-(5-methylisoxazol-3-yl)-urea (PNU-120596) and 3a,4,5,9b-tetrahydro-4-(1-naphthalenyl)-3H-cyclopentan[c]quinoline-8-sulfonamide (TQS) (Gronlien et al., 2007).

1,4-diazabicyclo[3.2.2]nonan-4-yl(5-(3-(trifluoromethyl)-phenyl)-furan-2-yl)methanone hydrochloride (NS6740) is a silent agonist able to modulate the cholinergic anti-inflammatory pathway with both in vitro (Thomsen and Mikkelsen, 2012) and in vivo models (Papke et al., 2015). NS6740 is particularly effective at producing prolonged desensitization of α_7 receptors (Papke et al., 2018a), suggesting that the non-conducting states induced by NS6740 are the active states for controlling the cholinergic anti-inflammatory pathway (Papke et al., 2015).

The earliest models for a silent agonist binding site assumed it to be an extension of the canonical orthosteric agonist binding site recognized by acetylcholine. Recently, additional insights into silent agonism have implicated an alternative allosteric agonist binding site in the extracellular vestibule of the receptor (Gulsevin et al., 2019), first identified as being one of two binding sites recognized by the allosteric agonist-positive allosteric modulator (ago-PAM) (3aR,4S,9bS)-4-(4-bromophenyl)-3a,4,5,9b-tetrahydro-3H-cyclopenta[c]quinoline-8-sulfonamide (GAT107); the other site is within the transmembrane domains and shared with PAMs such as PNU-120596 and TQS (Papke et al., 2014). The identification of the novel extracellular allosteric agonist binding site relied on the use of an α_7 C190A mutant, which is unresponsive to acetylcholine or other typical orthosteric agonists, even when combined with

PNU-120596 or TQS. The α_7 C190A mutant receptors are, however, very effectively activated by GAT107 or by the silent agonist 1,1-diethyl-4(naphthalene-2-yl)piperazin-1-ium iodide (2NDEP) combined with PNU-120596 (Gulsevin et al., 2019). The activation could be blocked by cis-trans-4-(2,3,5,6-tetramethylphenyl)-3a,4,5,9b-tetrahydro-3H-cyclopenta[c]quinoline-8-sulfonamide (TMP-TQS), a compound characterized as a selective antagonist of the direct allosteric activation by GAT107 (Horenstein et al., 2016; Papke et al., 2020b). While the silent agonism of 2NDEP appears to arise primarily through activity at the allosteric agonist site, other silent agonists in the 1,1-diethyl-4-phenylpiperazinium (diEPP) family appear to work at both the orthosteric and allosteric agonist binding sites (Gulsevin et al., 2019).

We recently published a series of NS6740 fragments (Pismataro et al., 2020) and analogs to explore the special structure-activity relations of this silent agonist. Here we investigate the mechanism of NS6740 in greater detail, model the interactions of NS6740 at both the orthosteric and the putative allosteric agonist binding sites, and evaluate the activity of NS6740 with the α_7 C190A mutant along with mutational analysis of the α_7 S36 residue, which is located in the orthosteric binding site.

2. Materials and methods

2.1. Reagents

Acetylcholine chloride, atropine, and other chemicals were purchased from Sigma-Aldrich Chemical Company (St. Louis, MO). NS6740 (Pismataro et al., 2020), GAT107 (Kulkarni & Thakur, 2013; Thakur et al., 2013), TMP-TQS (Papke et al., 2020b), and PNU-120596 (Williams

et al, 2011b) were synthesized as described previously. All compounds were confirmed by NMR to have a purity ≥ 95%. Fresh acetylcholine stock solutions were made in Ringer's solution each day of experimentation. Stock solutions of the PAMs were made in DMSO and kept at -20 ºC and diluted in Ringer's solution each day.

2.2. Heterologous expression of nicotinic acetylcholine receptors in Xenopus laevis oocytes

The human α_7 nicotinic acetylcholine receptor clone was obtained from Dr. J. Lindstrom (University of Pennsylvania, Philadelphia, PA). The human resistance-to-cholinesterase 3 (RIC-3) clone, obtained from Dr. M. Treinin (Hebrew University, Jerusalem, Israel), was co-injected with α_7 to improve the level and speed of α_7 receptor expression without affecting the pharmacological properties of the receptors (Halevi et al., 2003). Subsequent to linearization and purification of the plasmid cDNAs, cRNAs were prepared using the mMessage mMachine in vitro RNA transfection kit (Ambion, Austin, TX). Mutations in the α_7 receptor were introduced using the QuikChange Site-Directed Mutagenesis kit (Agilent, Santa Clara CA). The α_7C190A mutation was made in a C116S mutant to prevent spurious disulfide bond formation with the free cysteine at 191.

Oocytes were surgically removed from mature *Xenopus laevis* frogs (Nasco, Ft. Atkinson, WI) and injected with appropriate nicotinic acetylcholine receptor subunit cRNAs as described previously (Papke and Stokes, 2010). Frogs were maintained in the Animal Care Service facility of the University of Florida, and all procedures were approved by the University of Florida Institutional Animal Care and Use Committee (application approval number 202002669). In brief, the frog was first anesthetized for 15-20 min in 1.5 L frog tank water containing 1 g of 3-

aminobenzoate methanesulfonate buffered with sodium bicarbonate. The harvested oocytes were treated with 1.25 mg/ml collagenase (Worthington Biochemicals, Freehold, NJ) for 2 h at room temperature in calcium-free Barth's solution (88 mM NaCl, 1 mM KCl, 2.38 mM $NaHCO_3$, 0.82 mM $MgSO_4$, 15 mM HEPES, and 12 mg/l tetracycline, pH 7.6) to remove the follicular layers. Stage V oocytes were subsequently isolated, each injected with 50 nl containing 4 ng α_7 nicotinic acetylcholine receptor subunit cRNA and 2 ng RIC-3 cRNA, then maintained in Barth's solution with 0.32 mM $Ca(NO_3)_2$ and 0.41 mM $CaCl_2$. Recordings were carried out 1-7 days after injection.

2.3. Two-electrode voltage clamp electrophysiology

Experiments were conducted at room temperature (24 °C) using OpusXpress 6000A (Molecular Devices, Union City, CA) (Papke and Stokes, 2010). Both the voltage and current electrodes were filled with 3 M KCl. Unless otherwise indicated, oocytes were voltage-clamped at -60 mV. The oocytes were bath-perfused with Ringer's solution (115 mM NaCl, 2.5 mM KCl, 1.8 mM $CaCl_2$, 10 mM HEPES, and 1 μM atropine, pH 7.2) at 2 ml/min. Drug applications were 12s in duration followed by a 181 s washout period. Solution exchange typically occurs with a time constant of about 5 s, although washout may be uneven around the entire surface of the oocyte (Papke and Papke, 2002; Papke and Thinschmidt, 1998). For standard experiments, recordings for each oocyte constituted two initial control applications of acetylcholine and then an experimental compound applied alone or co-applied with acetylcholine or a PAM. Every experiment began with 8 cells (the capacity of the recording system); however, due to the nature of the experiments, not all cells remained viable through entire experiments, and some cells had

large responses that could not be adequately voltage clamped. Therefore, n varied from 4 to 8. The control acetylcholine concentration was 60 µM. The responses were calculated as both peak current amplitudes and net charge, as previously described (Papke and Papke, 2002). The average responses of the two initial acetylcholine controls from each cell were used for normalization.

Data for standard experiments at the fixed holding potential of -60 mV were filtered at 20 Hz, sampled at 50 Hz, and analyzed by Clampfit 10.3 (Molecular Devices) and Excel (Microsoft, Redmond, WA). Data were expressed as means ± S.D. from at least four oocytes for each experiment and plotted by Kaleidagraph 4.5.2 (Synergy Software, Reading, PA). Type II PAMs produce extremely large increases (>100,000-fold) in the single-channel currents of a small fraction of the receptors (≤ 1%), so they are intrinsically variable in amplitude and duration (Williams et al, 2011b), making it difficult to identify truly "representative" responses. Therefore, we display multi-cell averages for comparisons of these complex responses. The averages of normalized data were calculated using an Excel (Microsoft) template for each of the 10,500 points in each of the 210 s traces (acquired at 50 Hz). Following subtraction of the basal holding current, data from each cell, including the acetylcholine controls, were normalized by dividing each point by the peak of the acetylcholine control from the same cell. The normalized data were then averaged and standard errors of the mean (S.E.M.) for the multi-cell averages calculated on a point-by-point basis. The dark lines in the figures represent the average normalized currents and the shaded areas the range (±) of the S.E.M. of the averaged raw data at each of the point in the trace. Scale bars of averaged traces reflect the scaling factor relative to the average peak current amplitude of the acetylcholine controls used for the normalization procedures. These plots (Stokes et al., 2019) illustrate the differences in peak currents, net

charge, the kinetics of the responses, and the variability throughout the entire time course of the responses.

2.4. Docking experiments

The homology model of the human α_7 nicotinic acetylcholine receptor was generated as recently described (Gulsevin et al., 2019). Note that the modeling process was performed without imposing fivefold symmetry, thus obtaining an asymmetric final homology structure composed of 1020 total amino acids, uniformly distributed in the five subunits A, B, C, D, and E named in a counter-clockwise direction as viewed from the top of the channel. The binding pocket was localized at the interface between two different subunits; these interfaces were identified as I_{AB}, I_{BC}, I_{CD}, I_{DE}, and I_{EA}, where the first letter represented the primary face and the second letter the complementary face. Given the non-symmetric model, docking calculations were run at all five interfaces. In order to define the docking space, we used a grid large enough to cover a wider portion, including the orthosteric agonist binding site as well as the direct allosteric binding site in the vestibular side (Horenstein et al., 2016; Gulsevin et al., 2019; Papke et al., 2014).

The ligands investigated were hand-drawn with MolView and structurally adjusted and protonated using Molden 5.0 (Schaftenaar et al., 2000). The final ensuing structures were then optimized in their geometry employing HF/6-31G* optimization followed by B3LYP/6-31G** optimization (Gaussian 09). Generated potential output files were converted to .mol2. Employing Schrödinger Suite 2004-2 (Friesner et al., 2006), ligand preparation was carried out with LigPrep program: the possible states were generated at target pH 7 ± 2 using Epik, and for each compound three low-energy ring conformations were generated. Upon preparation, the ligands

were docked on each interface of Homology Model 2 (HM2). Glide XP (Friesner et al., 2006) was used and the following conditions were set up: flexible ligand sampling, addition of Epik state penalties to docking score, rewarding of intramolecular hydrogen bond, enhancement of conjugated pi atom planarity, and application of post-docking minimization, with a maximum of 10 poses per ligand. All poses were ranked based on docking score, and only protonated forms were considered for the analysis since the high pKa value of the tertiary amine in the diazabicyclic system argues for protonation at physiological pH, and active nicotinic orthosteric ligands require a positive charge (Hibbs et al., 2009). The poses are visually interpreted based on their electrostatic, hydrogen, and hydrophobic interactions.

3. Results

3.1. Partial agonism of α_7 by NS6740

Although originally characterized as a silent agonist of α_7 (Briggs et al., 2009; Papke et al., 2015), NS6740 is more accurately a weak partial agonist showing a maximal efficacy of approximately 20 % that of acetylcholine at a concentration of 30 µM (Pismataro et al., 2020). Although in a full concentration-response study (Fig. 1A) responses of this magnitude were observed over a relatively wide range of concentrations (1 - 100 µM), responses were smaller with the application of either higher or lower concentrations of NS6740, yielding an inverted-U curve. This curve could be well fit (Chi-square = 0.00074, R = 0.982) to a function that was the product of an activation curve, defined by the Hill equation with a positive slope, and an inhibitory function with a negative Hill coefficient of -1.

3.2. Inhibition of acetylcholine responses following NS6740 applications

Consistent with producing both activation and long-lived antagonism (desensitization) of α_7 responses (Papke et al., 2018a), we observed an inhibition of acetylcholine control responses obtained after NS6740 application (Fig. 1B). This inhibition curve was well fit (Chi-square = 0.0056, R = 0.99785) by an inverse Hill function with Hill coefficient of -0.97 ± 0.1 and an IC_{50} of 8.7 ± 1.2 µM.

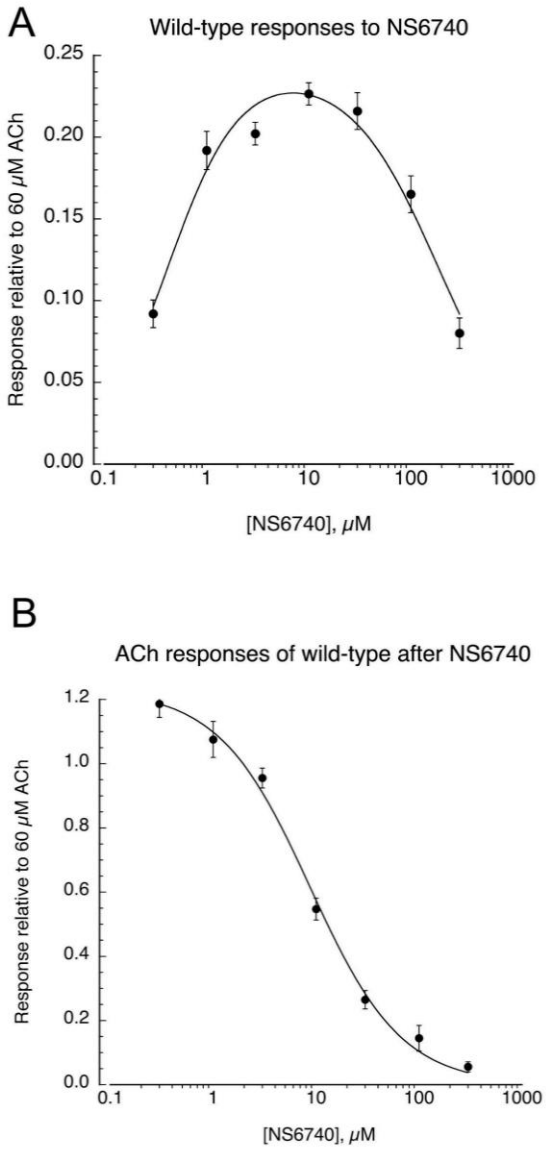

Fig. 1. Concentration-response data for NS6740 activation and inhibition of α_7. **(A)** Net-charge responses calculated relative to the average of two 60 μM acetylcholine controls delivered prior to the NS6740 application. Note that 60 μM acetylcholine is approximately the EC_{80} relative to acetylcholine maximum. Plotted are the averages ± S.E.M. of 7-8 oocytes at each concentration (n = 7 at 100 μM, n = 8 at the other concentrations). The data were fit using the Levenberg–Marquardt algorithm to the product of an activation function defined by the Hill equation and an inhibition function with a Hill slope of -1 (Chi-square = 0.00074, R = 0.982). The EC_{50} for activation was 420 ± 96 nM, with an I_{max} = 0.24 ± 0.02. The

IC_{50} for inhibition was 182.06 ± 52 µM. **(B)** The inhibition of acetylcholine control responses following NS6740 applications. Concentration-response function for the observed decreases in acetylcholine control net-charge responses following NS6740 applications. Plotted are the averages ± S.E.M. of 7-8 oocytes at each concentration. The data were fit using the Levenberg–Marquardt algorithm to a Hill equation with a negative Hill slope (Chi-square = 0.0056, R = 0.99785), n_H = -0.98 ± 0.10 and IC_{50} = 8.7 ± 1.2 µM.

3.3. PAM-reversible desensitization of acetylcholine responses following NS6740 applications

Consistent with the hypothesis that the reduced acetylcholine responses following NS6740 were due to the stable induction of desensitization, applications of the type II PAM PNU-120596 alone after NS6740 produced large responses (Fig. 2).

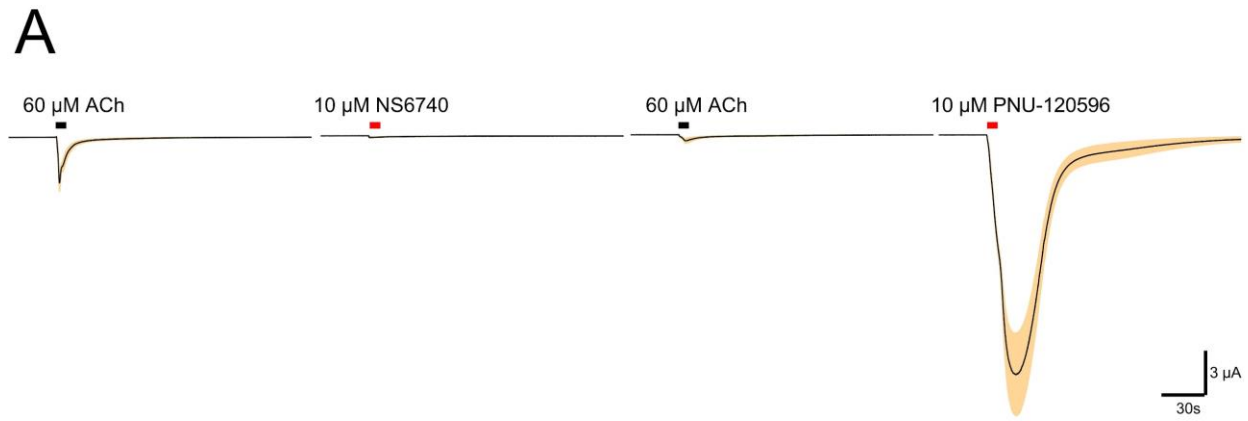

Fig. 2. Inhibition of acetylcholine responses is associated with the induction of PAM-sensitive desensitization. Shown are the averaged responses (black lines) of seven cells (± S.E.M., shaded areas) to control applications of 60 µM acetylcholine, followed by 10 µM NS6740, a subsequent application of 60 µM acetylcholine, and then the application of 10 µM PNU-120596, at four-minute intervals. Prior to

averaging, responses from each cell were normalized to the amplitude of the first acetylcholine control obtained from the same cell.

3.4. PAM-enhancement of NS6740 partial agonism

As expected, the co-application of 10 µM PNU-120596 with NS6740 increased the magnitude of the responses measured as net charge (Papke and Papke, 2002) (Fig. 3). Interestingly this was also an inverted-U function that could be fit as the product of both an activation (EC_{50} = 0.06 ± 0.05 µM, I_{max} = 47.9 ± 15.35) and inhibition (IC_{50} = 5.9 ± 4.8 µM) function, although due to the large variability typical of PAM-potentiated currents, the Chi-square value of the fit (302, r = .934) was large.

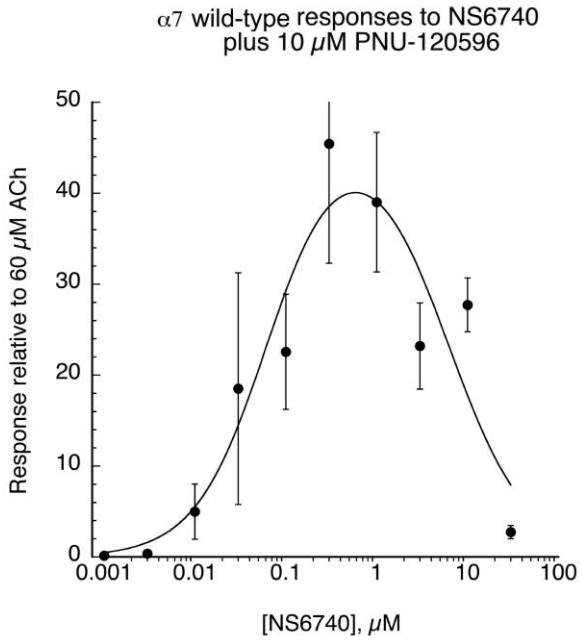

Fig. 3. Concentration-response data for NS6740 activation of α_7 when co-applied with 10 µM PNU-120596. Net-charge responses were calculated relative to the average of two 60 µM acetylcholine controls delivered prior to the NS6740 application. Plotted are the averages ± S.E.M. of 7-8 oocytes at each concentration. The data were fit using the Levenberg–Marquardt algorithm to the product of an activation function defined by the Hill equation and an inhibition function with a Hill slope of -1 (Chi-square = 0.00074, R = 0.982). The EC_{50} for activation was 0.06 ± 0.05 µM, with an I_{max} = 47.9 ± 15.35. The IC_{50} for inhibition was 5.9 ± 4.8 µM.

3.5. PAM-dependent activation of the non-orthosterically activatible α_7 C190A receptor

The α_7 C190A mutant, due to a disruption of the vicinal disulfide at the tip of the C-loop in the orthosteric agonist binding site, is insensitive to activation by acetylcholine even when co-applied with PNU-120596 (Gulsevin et al., 2019). We have previously used this mutant to identify silent agonists that appear to produce PAM-dependent activation of α_7 by binding to the allosteric agonist site (Gulsevin et al., 2019), which is used by the ago-PAM GAT107 (Horenstein et al., 2016). No responses were observed when NS6740 was applied alone to C190A receptors across a range for concentration from 30 nM to 300 µM (data not shown). In order to determine whether the allosteric agonist binding site present in C190A may be important for PAM-dependent activation by NS6740, we co-applied NS6740 and 10 µM PNU-120596 to α_7 C190A mutants (Fig. 4). For these experiments, we used 1 µM GAT107 as reference stimulus for allosteric activation. Although 3 µM NS6740 co-applied with 10 µM PNU-120596 did not stimulate C190A receptors, co-applications with 10 or 30 µM NS6740 activated these receptors. These responses were fully blocked by co-applications of 100 µM of the allosteric antagonist TMP-TQS (Papke et al., 2020b), suggesting that NS6740 may function at the allosteric agonist

site. Additionally, it should be noted that if 30 µM NS6740 was applied to the C190A mutant, a subsequent application of 10 µM PNU-120596 alone produced no activation (data not shown), suggesting that NS6740 did not produce stable desensitization of this mutant.

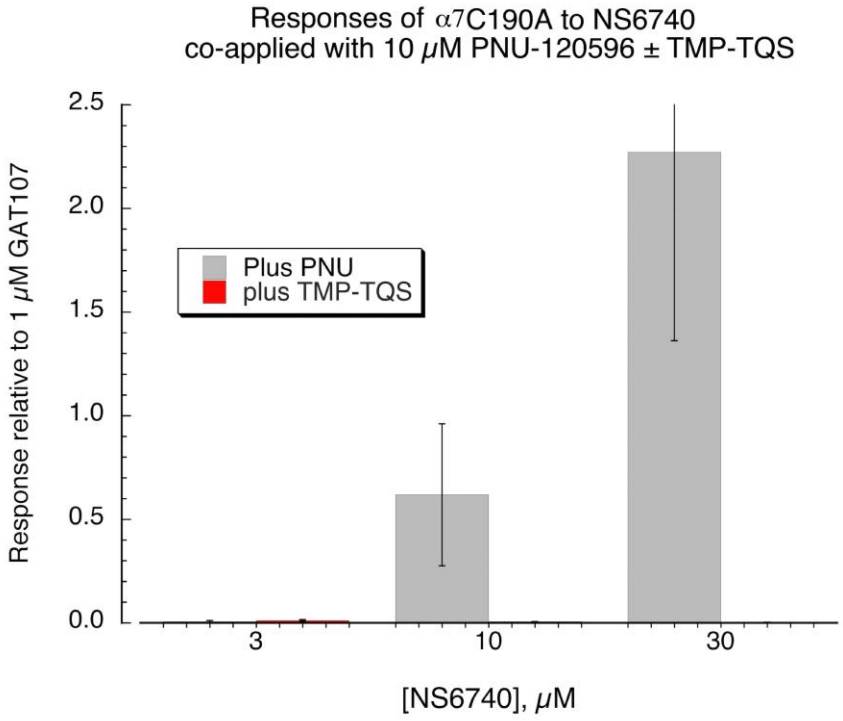

Fig. 4. Responses of α_7C190A mutant receptors to applications of NS6740 plus 10 µM PNU-120596 with or without co-application of 100 µM of racemic TMP-TQS (Papke et al., 2020b). Data are the averaged responses (± S.E.M.) from 6-8 cells under each condition. Although α_7C190A mutant receptors are unresponsive to acetylcholine, even when co-applied with PNU-120596, they respond well to the ago-PAM GAT107 (Gulsevin et al., 2019; Horenstein et al., 2016), so data were normalized to 1 µm GAT107 responses obtained on the same day.

3.6. Voltage-dependent channel block as a potential activity limiting responses to NS6740

We observed inverted-U concentration-response curves for both activation by NS6740 alone or in combination with PNU-120596, as well as inhibition of acetylcholine responses after NS6740 application. To test whether a factor limiting acetylcholine responses after NS6740 applications might be voltage-dependent channel block, we applied 10 µM NS6740 at +50 mV and compared the acetylcholine responses after application at this depolarized potential to responses after 10 µM applications at our standard holding potential of -60 mV (Fig. 5A). There was strong inhibition after the application of NS6740 at +50 mV ($P < 0.001$, corrected for multiple comparisons (Aickin and Gensler, 1996)). Although the inhibition after the application of NS6740 at +50 mV was somewhat less than after applications at -60 mV, the difference, after correction for multiple comparisons (Aickin and Gensler, 1996), was not significant at the $P < 0.05$ level.

Whereas the responses of wild-type α_7 responses in the absence of allosteric modulators are strongly inward rectifying (Miller et al., 2020; Seguela et al, 1993), a feature that prevented us from measuring the effects of voltage directly on responses to NS6740 alone, currents potentiated by modulators like PNU-120596 have linear current-voltage relationships (Miller et al., 2020; Peng et al., 2013; Sitzia et al, 2011). Therefore, we were able to directly compare the response of both wild-type α_7 (Fig. 5B) and the α_7C190A mutants (Fig. 5C) to application of 30 µM NS6740 co-applied with 10 µM PNU-120596 at different voltages. Responses of wild-type receptors were normalized to the average peak-current responses to control applications of 60 µM acetylcholine obtained from the same cells prior to averaging the raw data. The average net charge of the outward currents of wild-type α_7 responses obtained at +50 mV were nearly twice

as large as the inward current obtained at -60 mV ($P < 0.05$). Responses of C190A receptors were normalized to current responses to control applications of 1 μM GAT107 applied to the same cells prior to the application of 30 μM NS6740 co-applied with 10 μM PNU-120596. Although the currents obtained at +50 mV appeared larger (Fig. 5C), the difference was not statistically significant. However, visual inspection of the currents suggests that responses may have been delayed at the -60 mV holding potential.

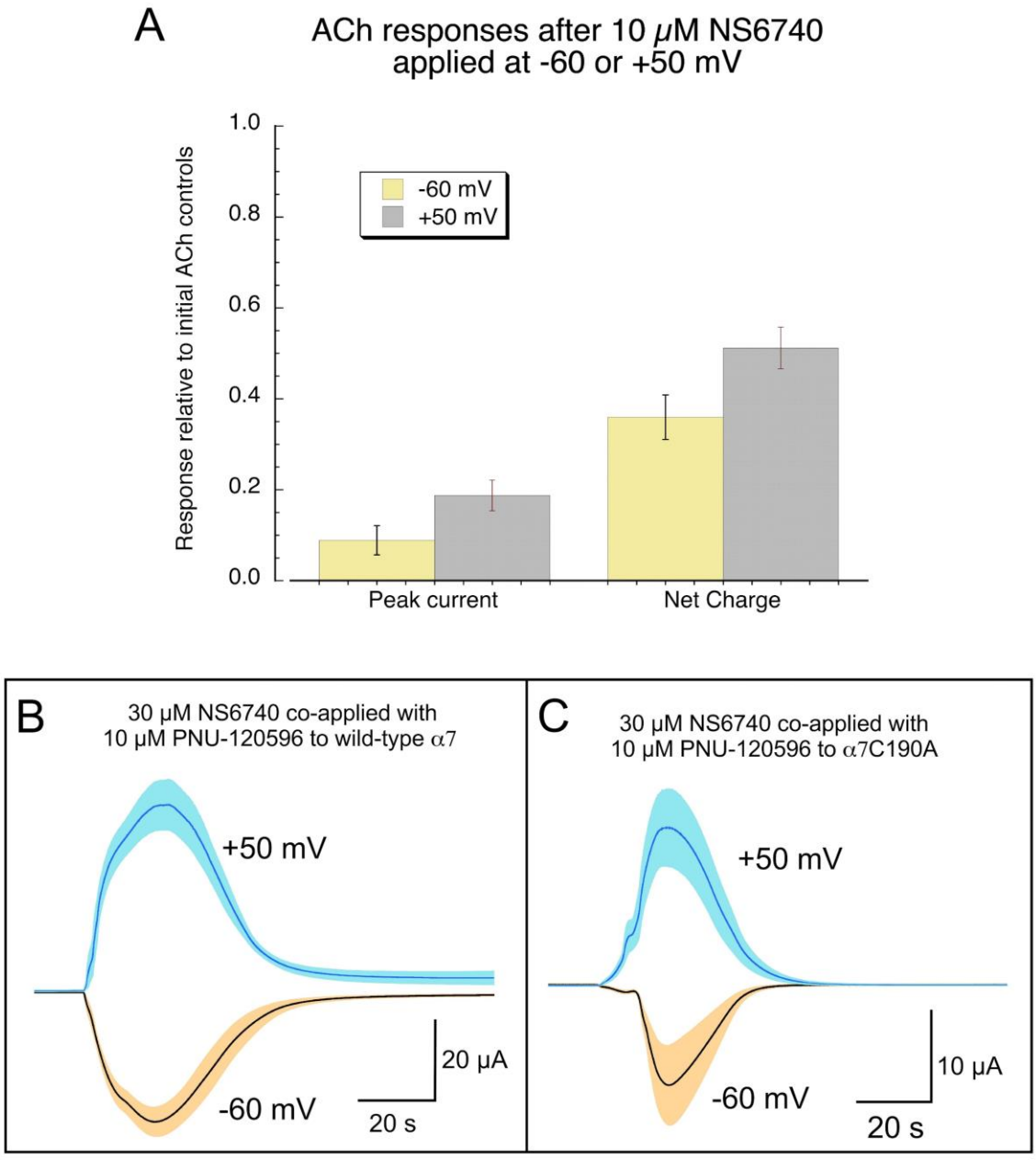

Fig. 5. Voltage-dependent channel block as a factor limiting responses to NS6740. **(A)** Effects of membrane voltage on the inhibition of acetylcholine responses by NS6740. During the delivery of 10 μM NS6740, cells were voltage-clamped at either the normal holding potential of -60 mV (n = 8) or at the depolarized potential of +50 mV (n = 8). **(B)** Averaged responses (solid lines, ± S.E.M. shaded areas, n = 5) of wild-type α_7 receptors to applications of 30 μM NS6740 co-applied with 10 μM PNU-120596,

obtained at either the standard holding potential of -60 mV (black and tan) or the depolarized potential of +50 mV (dark and light blue). **(C)** Averaged responses (solid lines, ± S.E.M. shaded areas, n = 5) of α_7 C190A receptors to applications of 30 µM NS6740 co-applied with 10 µM PNU-120596, obtained at either the standard holding potential of -60 mV (black and tan) or the depolarized potential of +50 mV (dark and light blue).

3.7. Docking studies at the orthosteric and allosteric activation sites of the α_7 nicotinic acetylcholine receptor

To gain insight into the potential interactions of NS6740 with the binding sites of α_7 nicotinic acetylcholine receptor, the compound was docked into an α_7 nicotinic acetylcholine receptor extracellular domain homology model (Gulsevin et al, 2020; Li et al., 2011). It is tempting to assume that the binding sites at the subunit interfaces in α_7 subunit complexes are equivalent, and this appeared to be the case in the published static structure with epibatidine bound at all of the sites (Noviello, 2021). However, this is not likely to be the case once ligand binding occurs at single sites and the receptor undergoes the dynamic conformational changes associated with activation and desensitization. It was in fact shown in crystal structures of the AChBP bound to the partial agonist GTS-21 (Hibbs, 2009), that the ligand was found bound in different orientations at select interfaces. We have also previously observed non-equivalence in the five subunit interfaces (Gulsevin, 2019) in dynamic simulations with our model that is based on a humanized α_7 AChBP analog (Li, 2011). Therefore, the homology model we used was created without enforced symmetry between each of the subunits, yielding non-equivalence of the sites around the receptor on the nanosecond time scale. Consistent with previous studies, (Chiodo et al, 2017; Henchman et al, 2003; Law et al, 2005), this model of the receptor shows

differences in the local conformations of each chain of the homopentamer. Thus, each subunit interface may be considered unique (Gulsevin et al, 2020). We designate the five subunits A, B, C, D, and E, and their corresponding interfaces I_{AB}, I_{BC}, I_{CD}, I_{DE}, and I_{EA}. NS6740 was docked into the receptor in the (+1) charge state at all five receptor interfaces. Both orthosteric and allosteric agonist binding sites are found at the subunit interfaces, but the allosteric site is inside the vestibule (Gulsevin et al., 2019; Spurny et al., 2015), whereas the well-known orthosteric site is external to the vestibule (Horenstein et al., 2016; Li et al., 2011; Papke et al., 2014). The docking of NS6740 gave different results based on the specific interface involved (Supporting Information, Table S1). In detail, docking into interfaces I_{AB} and I_{EA} always showed NS6740 binding to the orthosteric site, while docking into I_{DE} displayed allosteric binding site poses. Mixed poses at both orthosteric and allosteric sites were obtained at I_{BC} and I_{CD}. In general, a better docking score was associated with binding at the orthosteric site(s). Docking score is an empirical scoring function that roughly approximates the ligand binding free energy and allows classifying compounds based on their binding affinity.

Fig. 6A shows NS6740 bound at the various subunit interfaces of the α_7 nicotinic acetylcholine receptor model.

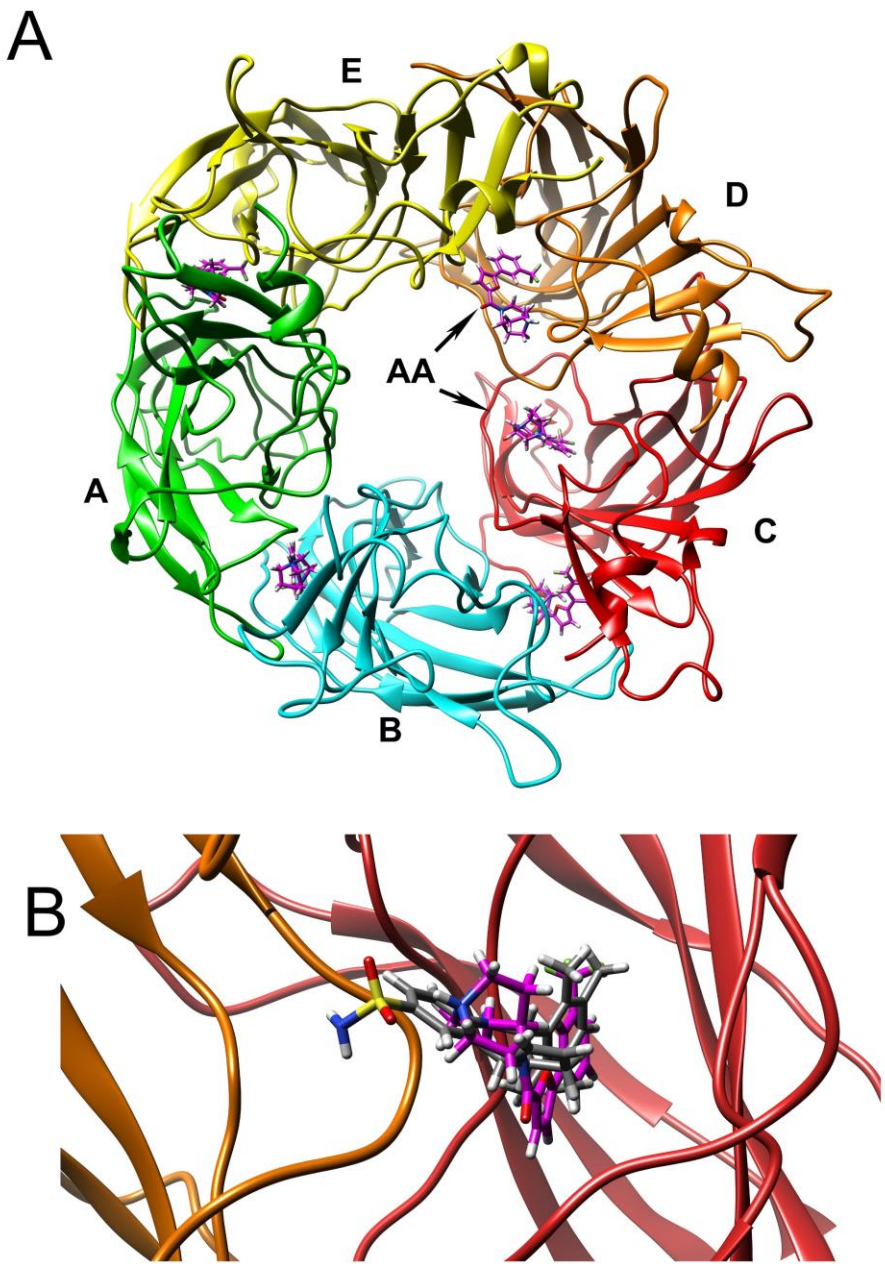

Fig. 6. NS6740 binding sites in α_7. **(A)** NS6740 bound in the α_7 nicotinic acetycholine receptor homology model (Gulsevin et al., 2019). Viewed from the top and in the counterclockwise direction: subunit A is green, subunit B is light cyan, subunit C is red, subunit D is orange, and subunit E is yellow. NS6740, exhibited in magenta, is shown with orthosteric placement at AB, BC, and EA interfaces, and allosteric binding poses are shown at CD and DE interfaces. AA = allosteric activation site. **(B)** The superposition of NS6740 and (-)TMP-TQS docked into the allosteric agonist site at the CD interface. Chain C is in red,

Chain D is in orange. The carbon backbone of NS6740 is colored magenta, the carbon backbone of (-)TMP-TQS is gray. The polar ends of both molecules point into the vestibule. Amino acid side chains are not shown for clarity. Consult Table S2 for details on amino acid contacts**.**

3.8. Molecular Modeling of the putative allosteric binding site

Recent findings support the idea that some very weak and silent agonist compounds might alternatively bind to the allosteric agonist site to produce PAM-dependent activation. This site is bound by the ago-PAM GAT107 and is responsible for the allosteric activation of α_7 receptors by that ligand (Horenstein et al., 2016). The weak partial agonists 2NDEP and 1,1-diethyl-4-(4-(trifluoromethyl)phenyl)piperazin-1-ium iodide (*p*-CF_3-diEPP) were electrophysiologically confirmed to produce allosteric activation activity of the α_7 receptor. When computationally investigated, they both showed orthosteric agonist binding site poses at interfaces I_{AB}, I_{BC}, and I_{EA} and allosteric agonist site poses at I_{CD} and I_{DE} (Gulsevin et al., 2019), in line with our docking data obtained with NS6740. In light of these results, we analyzed the binding poses of NS6740 at the I_{CD} and I_{DE} interfaces in which the bicyclic amine was located at the polar mouth of the allosteric pocket and the *meta*-CF_3 end of the molecule deep within the non-polar pocket. Overall, most of the interacting amino acids are non-polar; Table S2 in Supporting Information presents a detailed list of amino acids interacting with bound NS6740.

We have previously characterized the allosteric antagonist (-)TMP-TQS and its likely binding to the allosteric agonist site in α_7 (Papke et al., 2020b). As shown in Fig. 6B, the docking of NS6740 to the allosteric site essentially overlapped with that of (-)TMP-TQS, consistent with the hypothesis that there would be a competitive binding of the two ligands at this site.

3.9. Molecular Modeling of the putative orthosteric binding site

Analyzing the docking results in terms of the energy score and the observed binding poses, we suggest that interface I_{AB} best describes the potential binding mode of NS6740 at the receptor orthosteric agonist site. The binding at this interface is supported not only by the best docking scores obtained, but also by the poses that are consistent with those described for known partial agonists (Hibbs et al., 2009). In detail, when NS6740 was docked into the orthosteric site of the α_7 nicotinic acetylcholine receptor, the positively charged diazabicyclic structure was located under the C-loop and embedded in the aromatic cage composed of key residues Tyr93, Trp149, Tyr188, and Tyr195 of the primary interface and Trp55 of the complementary interface. This group of aromatic side chains plays a central role in both ligand binding and binding stabilization.

According to the binding pose of NS6740 obtained from our docking studies (Fig. 7A), the protonated diazabicyclic nitrogen forms a hydrogen bond interaction with the carbonyl of Trp149 (subunit A of I_{AB}) and electrostatic π-cation interactions with Trp149 and Tyr195 (subunit A of I_{AB}). Moreover, the NS6740 carbonyl group establishes a hydrogen bond with the Gln57 (subunit B of I_{AB}) sidechain. The aromatic portion of NS6740 points under the C-loop, with furan and phenyl rings placed at a suitable distance for face-to-face aromatic π-π interactions with Trp55 (subunit B of I_{AB}). We found the trifluoromethyl group, known to be critical for the unique properties of NS6740 (Pismataro et al., 2020), to be within 3.45 angstroms of the S36 hydroxyl group (Fig. 7B). The substitution of a valine for the serine at this site reduced this distance to the point where it seemed likely that there would be a steric hindrance to NS6740 binding (Fig. 7C).

Based on these docking results, we were encouraged to perform electrophysiological investigations using a site-directed mutant of Ser36 to test the hypothesis that this residue is required to guide receptor binding interactions associated with the unique properties of NS6740.

To summarize, NS6740 might bind to the allosteric agonist sites at some of the subunit interfaces, and binding to these sites would likely be competitive with the allosteric antagonist TMP-TQS. Also, docking studies suggest binding of NS6740 in the orthosteric agonist site would likely involve interaction with the S36 residue, which was previously shown to have H-bond interactions that are required for the desensitization produced by benzylidene anabaseines (Isaacson et al, 2013). With the modeling studies indicating possible interactions at both classes of activation sites, the question remained whether the unique prolonged desensitization produced by NS6740 was due to binding at the orthosteric or the allosteric agonist sites. Below we report the results of experimental studies designed to address this question.

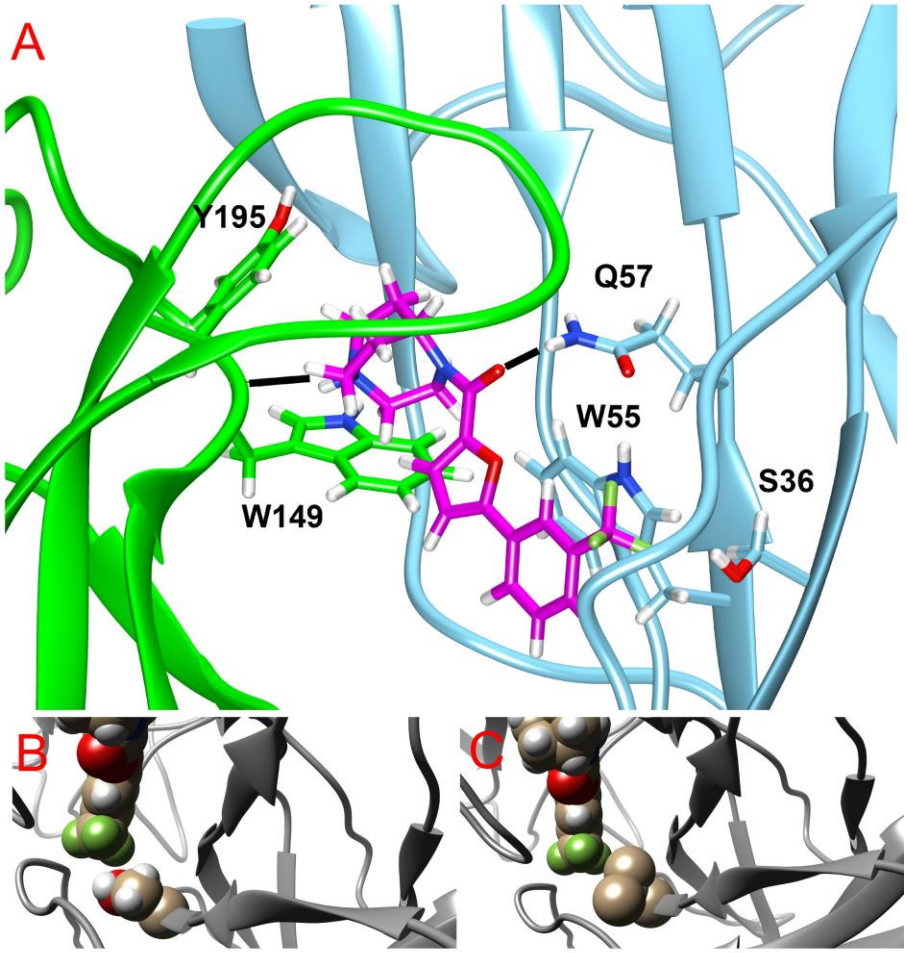

Fig. 7. Predicted binding mode of NS6740 in the α_7 orthosteric activation site. **(A)** The docking of NS6740 at the AB interface of the α_7 nicotinic acetycholine receptor homology model (Gulsevin et al., 2019). Subunit A is green and subunit B is light cyan. Selected key residues involved in ligand binding are displayed with carbon atoms colored green from subunit A and light cyan from subunit B. NS6740 is exhibited with its carbon atoms colored dark magenta. Oxygen atoms are red, nitrogen atoms blue, fluorine atoms green, and hydrogen atoms white. Hydrogen bonding interactions are indicated as black dashed lines. **(B)** Close-up of the docked ligand and the S36 residue. **(C)** Effect of serine-to-valine mutation on the fit of NS6740 in the orthosteric activation binding site of the AB interface.

3.10. TMP-TQS sensitivity of NS6740-primed activation by PNU-120596

To test the hypothesis that NS6740 binds to the allosteric agonist site to produce prolonged effects, we determined whether TMP-TQS would be able to block the NS6740-primed responses to applications of PNU-120596. As shown in Fig. 8, co-application of 30 µM (-)TMP-TQS (the more active isomer (Papke et al., 2020b) totally blocked responses to an application of PNU-120596. However, this inhibition was transient and did not perturb the desensitization induced by the initial application of NS6740 since cells treated with (-)TMP-TQS were as sensitive to a second PNU-120596 application as cells that received just two applications of the PAM. This suggests that even though NS6740 might bind at the allosteric agonist site, it is not having prolonged effects at that site since treatment with TMP-TQS, which does bind there (Papke et al., 2020b) did not disturb the prolonged desensitization as measured by the second application of PNU alone. These results are consistent with NS6740 binding at a second site, i.e. the orthosteric agonist site as the locus for producing long-term desensitization. These data also indicate that (-)TMP-TQS is not just a competitive antagonist of allosteric activation, but rather when bound functions as an inverse agonist of allosteric activation.

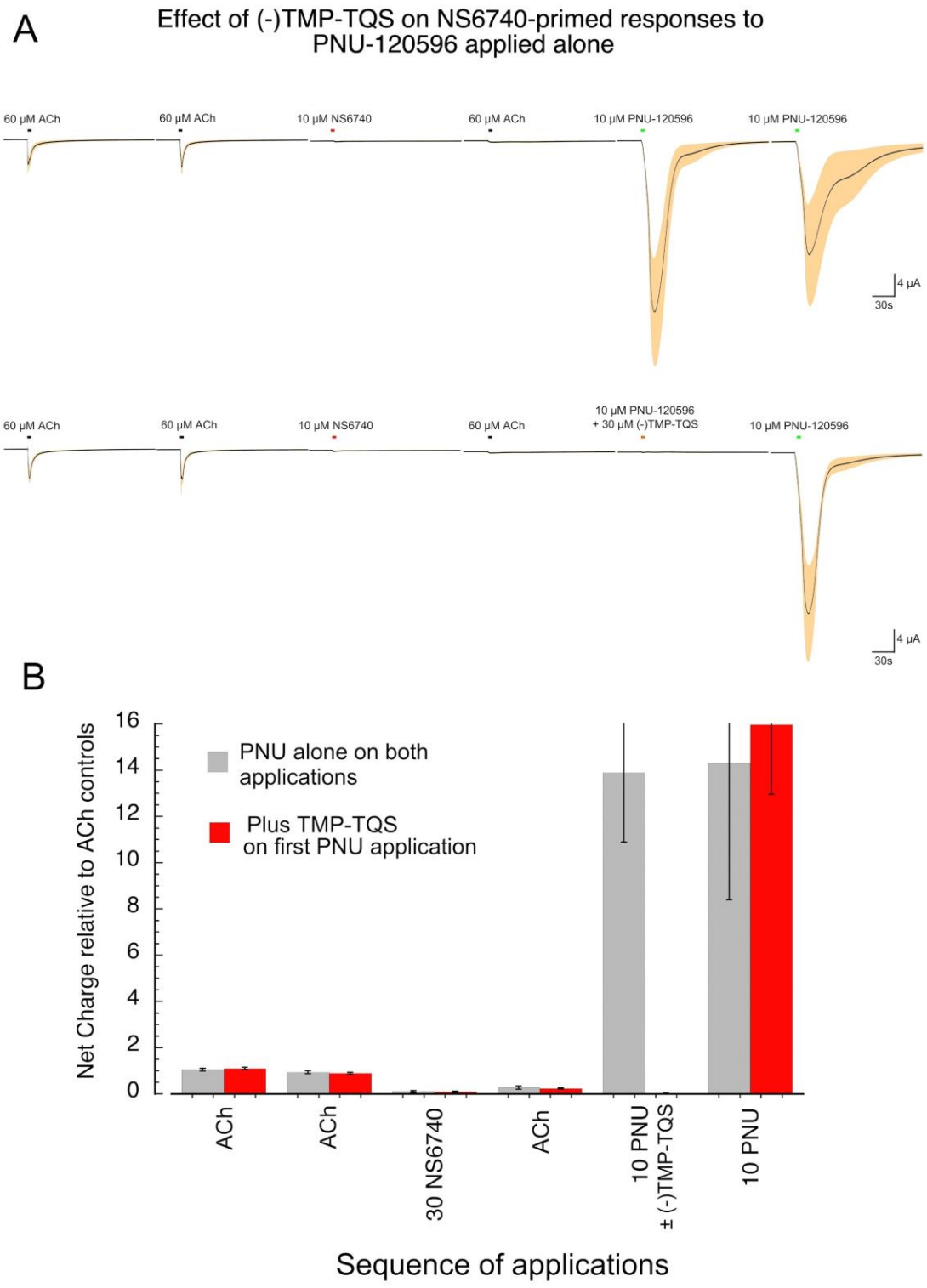

Fig. 8. TMP-TQS inhibition of NS6740-primed responses to PNU-120696. **(A)** Averaged responses (black lines) of seven cells (± S.E.M., shaded areas) to control applications of 60 µM acetylcholine,

followed by 10 µM NS6740, a subsequent application of 60 µM acetylcholine and then two applications of 10 µM PNU-120596, at four minute intervals. The upper traces (n = 5) are from cells receiving PNU-1205696 alone on the last two applications. The cells represented in the lower traces (n = 6) received 100 µM of the most active (-) isomer of TMP-TQS (Papke et al., 2020b) during the first application of PNU-120596. **(B)** Bar chart of the averaged net charge data (± S.E.M.) from the cells in **A**.

3.11. Requirement of S36 for NS6740 effects at the orthosteric binding site

In order to validate the details of the model for NS6740 docking to the orthosteric agonist binding site regarding the S36 residue, we tested the effects of NS6740 on the α_7S36V mutant, specifically to test whether the larger size of the valine would alter interactions that lead to activation and/or the induction of long-lived desensitization.

The α_7S36V mutants express somewhat smaller currents to applications of acetylcholine than wild-type receptors (Isaacson et al, 2013) but have acetylcholine concentration-response functions basically similar to wild-type receptors (Fig. 9). We note that with α_7S36V receptors NS6740 partial agonism is absent; there were no detectable responses at any concentration tested (Fig. 10A). Also, acetylcholine controls were not inhibited after NS6740 applications; in fact, at intermediate concentrations of NS6740, they were increased compared to the average of the two initial controls (Fig. 10A). There were also only small responses to PNU-120596 applied alone after NS6740 and the acetylcholine post-control applications (as with the protocol illustrated in Fig. 2). The largest PNU-120596 response, obtained after the 100 µM NS6740 application, was only 5% of the response with wild-type α_7 under the same conditions.

3.12. Activity of NS6740 at the allosteric agonist binding site in α_7S36V mutant receptors

While the modeling suggested specific effects of the S36V mutation at the orthosteric agonist site, the allosteric agonist binding site would be unaffected by this mutation. Therefore, in order to test whether NS6740 is able to couple with a PAM via binding to the allosteric agonist site, we co-applied NS6740 and PNU-120596 to α_7S36V mutant receptors. Although the effects of NS6740 at the orthosteric agonist binding site were compromised in α_7S36V mutants (Fig. 10A), co-applications of NS6740 with the PAM still produced significant activation in a concentration-dependent manner (Fig. 10B). As with wild-type α_7 receptors, the concentration dependence was described by an inverted U.

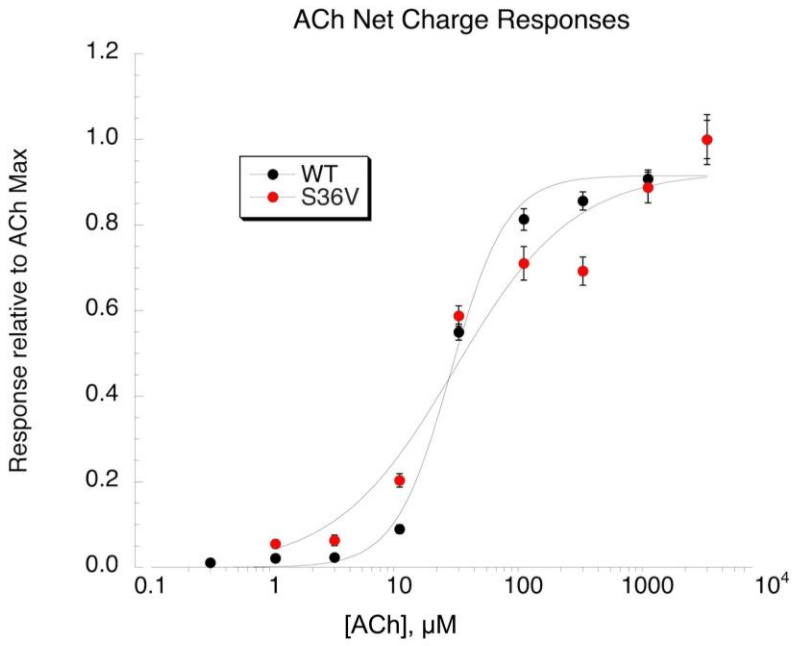

Fig. 9. Acetylcholine net-charge responses for α_7 wild-type and α_7S36V receptors (data from Isaacson et al., 2013). Net-charge responses were calculated relative to the average of two 60 µM acetylcholine controls. Plotted are the averages ± S.E.M. of 7-8 oocytes at each concentration and expressed relative to the acetylcholine maximum response for each receptor. The data were fit using the Levenberg–Marquardt algorithm to the product of an activation function defined by the Hill equation. The data for wild-type α_7 receptors were fit with a Hill slope of 1.94 ± 0.27 and an EC_{50} of 26 ± 2.7 µM (Chi-square = 0.014, R = 0.995). The data for α_7S35V receptors were fit with a Hill slope of 0.90 ± 0.38 and an EC_{50} of 27.7 ± 11.1 µM (Chi-square = 0.044, R = 0.977).

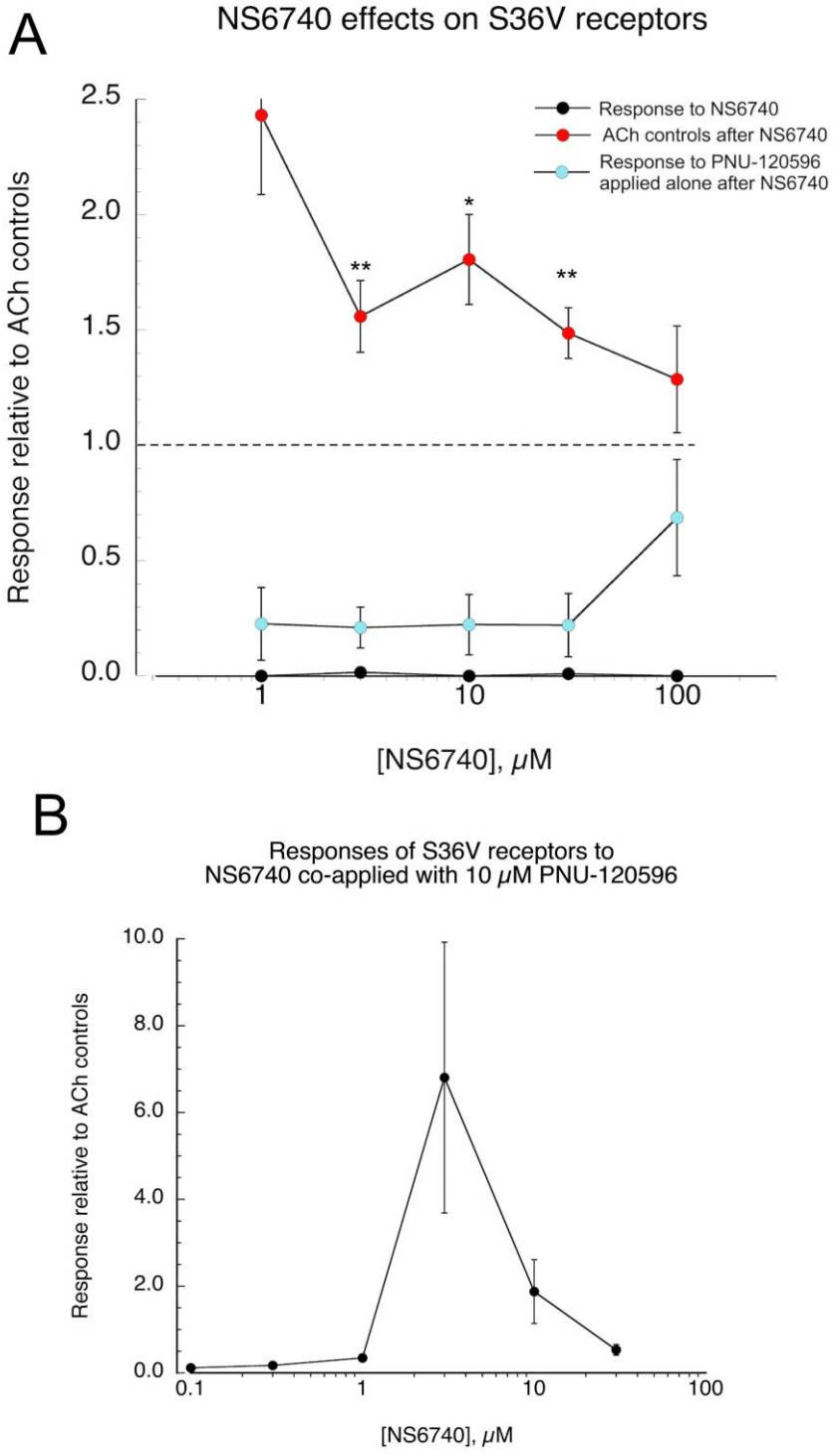

Fig. 10. NS6740 effects on α_7S36V receptors. **(A)** NS6740 was tested using a protocol similar to that illustrated in Fig. 2. The black symbols represent the NS6740-evoked responses of α_7S36V receptors.

Effectively, no responses were above our reliable limit of detection. The red symbols represent the acetylcholine control net-charge responses after the application of NS6740 at the concentrations indicated. The blue symbols represent responses to 10 µM PNU-120596 applied alone after the NS6740 and the acetylcholine. All data represent the average of 7-8 oocytes (± S.E.M.) normalized to the average of the two acetylcholine control responses obtained prior to the NS6740 applications. (Only one acetylcholine pre-control response is illustrated in Fig. 2). **(B)** NS6740 was co-applied to α_7S36V receptors with 10 µM PNU-120596 across a range of concentrations. Data represent the average of 7-8 oocytes (± S.E.M.) normalized to the average of the two acetylcholine control responses obtained prior to the test co-applications. Co-application of 3 µM NS6740 gave significant responses ($P < 0.05$) while co-applications at higher and lower concentrations gave lower responses, indicative of an inverted U relationship. However, the variability of the responses to 3 µM NS6740 plus PNU-120596 and the narrow range of effective concentration prevented the generation of a satisfactory curve fit.

4. Discussion

NS6740 is a unique modulator of α_7 nicotinic acetylcholine receptor activity, characterized by weak partial agonism and long-term stabilization of desensitized states that can be rendered conductive in the presence of a type II PAM. Our data suggest that, although NS6740 can have transient activity at the extracellular allosteric agonist binding site that is essential for activation by GAT107, the unique desensitizing activity of NS6740 relies on it binding to the orthosteric site shared with acetylcholine and other more efficacious agonists.

The amplitude and time course of macroscopic responses in a system like that used in these experiments is always a complex function of multiple simultaneous microscopic processes

including ligand binding, channel activation, channel inactivation, and desensitization, all sculpted by the process of solution exchange and washout (Papke, 2010). Our characterization of the partial agonist and desensitizing properties of NS6740 confirm previous studies (Papke et al., 2015; Papke et al., 2018a; Pismataro et al., 2020) and extend those findings to define the inverted-U curves associated with NS6740 activation, with and without the potentiating effects of PNU-120596.

The concentration of NS6740 critically impacts receptor behavior in both positive and negative ways since we show that the receptor responds with apparent inhibition at higher concentrations of NS6740. The concentration-dependent inhibition of acetylcholine responses following applications of NS6740 was also consistent with this idea, supporting the hypothesis that low concentrations of compound activated the receptor, but higher concentrations preferentially promoted entry into a long-lived desensitized state.

The hypothesis that channel block might be an additional factor limiting receptor responses at higher concentration was tested, and the data suggest that, although there might be a small amount of transient channel block, desensitization is more likely to be the major limiting factor. The persistence of the NS6740-induced desensitized state(s) is evidenced by the inhibition of acetylcholine response subsequent to a NS6740 application as well as a robust response to later applications of PNU-120596. Interestingly, the responses to co-application of NS6740 and PNU-120596 also displayed an inverted U, suggesting that at sufficiently high NS6740 concentration, the desensitized state shifts in nature to becoming PNU-120596 insensitive.

Docking studies suggested that NS6740 could be bound in either the classic orthosteric agonist site or the alternative allosteric agonist site. Although the electrophysiology data for NS6740 and its derivatives (Pismataro et al., 2020) are consistent with action at the orthosteric

agonist binding site, experiments with the α_7C190A acetylcholine-insensitive mutant revealed that responses to NS6740 co-applied with PNU-120596 also indicate functional activity at the allosteric agonist binding site. Consistent with activity at the allosteric site, responses of α_7C190A receptors to NS6740 plus PNU-120595 could be inhibited with co-application of TMP-TQS, which binds to the allosteric agonist site. An alternate interpretation of those data might be that TMP-TQS acts as an allosteric inhibitor, impacting the potentiated currents arising from NS6740 binding to the compromised orthosteric agonist site of α_7C190A. Further evidence for NS6740 effects at the allosteric agonist site were obtained with the α_7S36V mutant, which was selectively compromised in the NS6740 orthosteric site activity but was also still activatable by NS6740 co-applied with PNU-120596. Additionally, whether NS6740 is binding to the allosteric agonist site of α_7C190A or the altered orthosteric agonist site, it is apparent that NS6740 is not inducing stable desensitization in the mutant receptors since delayed applications produced no activation of α_7C190A receptors like they do in the α_7 wild-type receptors and very reduced responses in α_7S36V receptors (Fig. 10).

As shown in Fig. 8, wild-type α_7 receptors treated with NS6740 not only responded to delayed applications of PNU-120596, but these responses were completely blocked by (-)TMP-TQS. However, the inhibition was only transient since another subsequent application of PNU-120596 produced a full response. This result is not consistent with NS6740 exerting its activity through residence at the allosteric agonist site, but rather suggests that (-)TMP-TQS can function as an inverse agonist of allosteric activation associated with the PNU-120596 reversal of NS6740 desensitization associated with binding at the orthosteric agonist site.

Examination of poses of NS6740 docked into the orthosteric agonist site suggested that S36 was a critical position for NS6740 activity, and mutation of this residue indeed was highly

impactful on α_7 activity with NS6740 (but not acetylcholine)[1]. We observed loss of partial agonism for NS6740, loss of the inhibition of acetylcholine response in post-control acetylcholine applications, and weak response to co-application of NS6740 and PNU-120596. We therefore conclude that S36 is a critical location for function of NS6740 in terms of both partial agonism and induction of persistent desensitized states, so these experiments support the idea that the majority of activity seen for NS6740 is via action at the orthosteric agonist site of the receptor. The nature of the putative noncovalent interactions between S36 and the trifluoromethyl group are likely to be complex (Esterhuysen et al., 2017), but introduction of the S36V mutation appeared to impact NS6740 via steric impact of the bulkier valine side chain. It should be noted, though, that we modeled the NS6740 binding at a single orthosteric interface, the one that appeared to give the best binding, and that the effects of the S36 mutation might be different at other orthosteric agonist sites, perhaps accounting for the small residual effects of PNU-120596 application. Additionally, we are at a loss to explain the apparent increases in acetylcholine responses of α_7S36V receptors over a certain range of NS6740 concentrations.

As noted above, there may be multiple factors limiting the responses of wild-type α_7 receptors to NS6740, both applied alone and when co-applied with PNU-120596. Although

[1] It should be noted that the recently published α_7 structure (Noviello, 2021) is based on a sequence (GenBank accession number, AAA83561.1) that differs from the sequence of the clone used for our experiments provided by Dr. J Lindstrom (GenBank accession number, NM_000746.6, nucleotide; NP_000737.1, protein) and the eight human α_7 reference sequences in the NCBI protein database at two residues in the extracellular domain, most importantly position 36 where an asparagine is present rather than the serine found in other sequences (NP_000737.1, NP_001177384.1, XP_011519478.2, XP_011519479.1, XP_011519480.1, XP_016877371.1, XP_016877372.1, XP_016877373.1). The sequence used by Noviello et al. also has a proline at position 112 where other sequences have a serine.

we can fit both of the inverted-U curves to the product of separate activation and inactivation functions, there is no straight-forward interpretation of what those functions represent (Papke, 2010). Additionally, the curve-fit function that is the product of a positive and a negative process is not a unique solution (Papke, 2010). The intuition that the activating process dominates the rising phase of the function and the inactivating process is reflected in the decay may be entirely incorrect, as was discovered to be the case with sodium channel activation and inactivation (Aldrich et al., 1983). A further complication is that, as a partial agonist, there are intrinsic limitations to the NS6740 I_{max}, although typically for a partial agonist responses reach a stable plateau (Papke and Heinemann, 1994; Papke et al., 2011).

In the case of the inhibition of acetylcholine responses following NS6740 application, we can detect a single dominant inhibitory process with an apparent IC_{50} = 8.7 ± 1.2 µM. Interestingly, this may correspond to the negative function fit to the inverted-U curve of the responses to NS6740 plus PNU-120596 (IC_{50} = 5.9 ± 4.8 µM), suggesting that the same desensitization process may be limiting under both conditions. The relatively high apparent IC_{50} (182.06 ± 52 µM) limiting the responses to NS6740 applied alone may represent a different process, perhaps even reversible channel block.

The first published data on NS6740 (Briggs et al., 2009) identified it as what we classify as a "silent agonist" and focused on its action as an antagonist of the cognitive effects of the more efficacious α_7-selective agonist, A-582941. Similar data were published more recently reporting its effectiveness as an antagonist of the cognitive effects of the α_7 partial agonist BMS-902483 (Pieschl et al., 2017). Both of these observations most likely are due to the protracted desensitization of α_7 channel activation produced by NS6740, as is also likely to be the case with the report that NS6740 disrupts synaptic function in hippocampal brain slices (Papke et al.,

2018b). However, the potential clinical importance for NS6740 came to light with a study that demonstrated its effective reduction of LPS stimulated release of the pro-inflammatory cytokine TNF-alpha by microglia (Thomsen and Mikkelsen, 2012). This potential was later confirmed by in vivo studies that showed NS6740 induced significant dose- and time-dependent antinociceptive activity in formalin-model of inflammatory pain and chronic nerve constriction model of neuropathic pain. The antinociceptive activity of NS6740 in these models was demonstrated to be α_7-dependent. In addition, NS6740 administration reversed pain-induced aversion, an important affective component of pain (Papke, 2015).

5. Conclusions

Our results show that as NS6740 may promote transient PAM-dependent currents via the allosteric activation sites, the stable desensitization seen with wild-type α_7 receptors seems to rely on the orthosteric binding sites. Residue S36 in the orthosteric agonist binding site appeared to be important for NS6740 interaction; its mutation led to an impaired activity of NS6740. The results indicate that the unique properties of NS6740 are due primarily to the binding at the sites for orthosteric agonists. The NS6740 desensitizing properties are related to its anti-inflammatory activity, for which the modality channel activation appears to be nonessential (Bagdas et al., 2016; Horenstein and Papke, 2017; Papke et al., 2015). Recently, interest has shifted toward the role of α_7 receptors in regulating inflammatory disease and pain via the cholinergic anti-inflammatory pathway (Rosas-Ballina and Tracey, 2009). As noted above, both in vivo (Papke et al., 2015) and in vitro (Thomsen and Mikkelsen, 2012) data demonstrate the activity of NS6740 in modulating inflammation. It is likely that NS6740 is able to penetrate the brain, since it was

able to oppose the effects of other α_7 drugs that due to their channel efficacy might be less active modulators of microglial based brain inflammation (Briggs et al., 2009; Pieschl et al., 2017). Nonetheless, the challenge for future drug development will be to further dissect the functionality of specific elements of NS6740 with the goal of developing analogs that produce the desensitization associated with cholinergic anti-inflammatory pathway signaling (Pismataro et al., 2020).

Data availability

All original data can be made available upon request to the corresponding author.

Credit authorship contribution statement

Maria Chiara Pismataro: Research design, Investigation, New reagents and analytic tools contribution, Data analysis, Writing - review & editing. **Nicole A. Horenstein:** Research design, Investigation, Data analysis, Writing - review & editing. **Clare Stokes:** Research design, Investigation, Data analysis, Writing - review & editing. **Clelia Dallanoce:** Research design, New reagents and analytic tools contribution, Writing - review & editing. **Ganesh A. Thakur:** New reagents and analytic tools contribution. **Roger L. Papke:** Research design, Data analysis, Writing - review & editing, Supervision.

Declaration of competing interest

No author has an actual or perceived conflict of interest with the contents of this article.

Acknowledgments

This research was supported by the National Institutes of Health Grants: Institute of General Medical sciences [GM57481] (CS, NAH, RLP), and National Eye Institute [EY024717] (GAT). The University of Milan financed the doctoral position of MCP.

Appendix A. Supplementary data

Supplementary data to this article can be found online.

References

Aickin, M., Gensler, H., 1996. Adjusting for multiple testing when reporting research results: the Bonferroni vs Holm methods. Am. J, Public Health 86, 726-728.

Aldrich, R.W., Corey, D.P., Stevens, C.F., 1983. A reinterpretation of mammalian sodium channel gating based on single channel recording. Nature 306, 436-441.

Bagdas, D., Gurun, M.S., Flood, P., Papke, R.L., Damaj, M.I. 2018. New Insights on Neuronal Nicotinic Acetylcholine Receptors as Targets for Pain and Inflammation: A Focus on alpha7 nAChRs. Curr. Neuropharmacol. 16, 415-425.

Bagdas, D., Wilkerson, J.L., Kulkarni, A., Toma, W., AlSharari, S., Gul, Z., Lichtman, A.H., Papke, R.L., Thakur, G.A., Damaj, M.I., 2016. The alpha7 nicotinic receptor dual allosteric agonist and positive

allosteric modulator GAT107 reverses nociception in mouse models of inflammatory and neuropathic pain. Br. J. Pharm. 173, 2506-2520.

Briggs, C.A., Gronlien, J.H., Curzon, P., Timmermann, D.B., Ween, H., Thorin-Hagene, K., Kerr, P., Anderson, D.J., Malysz, J., Dyhring, T., Olsen, G.M., Peters, D., Bunnelle, W. H., Gopalakrishnan, M., 2009. Role of channel activation in cognitive enhancement mediated by alpha7 nicotinic acetylcholine receptors. Br. J. Pharmacol. 158, 1486-1494.

Cannon, C.E., Puri, V., Vivian, J.A., Egbertson, M.S., Eddins, D., Uslaner, J.M. 2013. The nicotinic alpha7 receptor agonist GTS-21 improves cognitive performance in ketamine impaired rhesus monkeys. Neuropharmacology 64, 191-196.

Castro, N.G., Albuquerque, E.X., 1995. a-Bungarotoxin-sensitive hippocampal nicotinic receptor channel has a high calcium permeability. Biophys. J. 68, 516-524.

Cecon, E., Dam, J., Luka, M., Gautier, C., Chollet, A.M., Delagrange, P., Danober, L., Jockers, R., 2019. Quantitative assessment of oligomeric amyloid β peptide binding to α_7 nicotinic receptor. Br. J. Pharmacol. 176, 3475-3488.

Chiodo, L., Malliavin, T.E., Maragliano, L., Cottone, G., 2017. A possible desensitized state conformation of the human alpha7 nicotinic receptor: A molecular dynamics study. Biophys. Chem. 229, 99-109.

de Jonge, W.J., Ulloa, L., 2007. The alpha7 nicotinic acetylcholine receptor as a pharmacological target for inflammation. Br. J. Pharmacol. 151, 915-929.

Di Cesare Mannelli, L., Pacini, A., Matera, C., Zanardelli, M., Mello, T., De Amici, M., Dallanoce, C., Ghelardini, C., 2014. Involvement of α_7 nAChR subtype in rat oxaliplatin-induced neuropathy: Effects of selective activation. Neuropharmacology, 79, 37-48.

El Nebrisi, E.G., Bagdas, D., Toma, W., Al Samri, H., Brodzik, A., Alkhlaif, Y., Yang, K.S., Howarth, F.C., Damaj, I.M., Oz, M., 2018. Curcumin Acts as a Positive Allosteric Modulator of α_7-Nicotinic

Acetylcholine Receptors and Reverses Nociception in Mouse Models of Inflammatory Pain. J Pharmacol Exp Ther. 365, 190-200.

Esterhuysen, C., Hesselmann, A., Clark, T., 2017. Trifluoromethyl: An Amphiphilic Noncovalent Bonding Partner. Chemphyschem. 18, 772-784.

Friesner, R. A., Murphy, R. B., Repasky, M. P., Frye, L. L., Greenwood, J. R., Halgren, T. A., Sanschagrin, P. C., Mainz, D. T., 2006. Extra Precision Glide: docking and scoring incorporating a model of hydrophobic enclosure for protein-ligand complexes. J. Med. Chem. 49, 6177−6196

Fucile, S., Renzi, M., Lax, P., Eusebi, F., 2003. Fractional Ca(2+) current through human neuronal alpha7 nicotinic acetylcholine receptors. Cell Calcium 34, 205-209.

Gronlien, J.H., Haakerud, M., Ween, H., Thorin-Hagene, K., Briggs, C.A., Gopalakrishnan, M., Malysz, J., 2007. Distinct profiles of alpha7 nAChR positive allosteric modulation revealed by structurally diverse chemotypes. Mol. Pharmacol. 72, 715-724.

Gulsevin, A., Papke, R.L., Horenstein, N.A., 2020. In silico modeling of the alpha7 nicotinic acetylcholine receptor: new pharmacological challenges associated with multiple modes of signaling. Mini Rev. Med. Chem. 20, 841-864.

Gulsevin, A., Papke, R.L., Stokes, C., Garai, S., Thakur, G.A., Quadri, M., Horenstein, N.A., 2019. Allosteric agonism of alpha7 nicotinic acetylcholine receptors: Receptor Modulation Outside the Orthosteric Site. Mol. Pharmacol. 95, 604-614.

Halevi, S., Yassin, L., Eshel, M., Sala, F., Sala, S., Criado, M., Treinin, M., 2003. Conservation within the RIC-3 gene family. Effectors of mammalian nicotinic acetylcholine receptor expression. J. Biol. Chem. 278, 34411-34417.

Henchman, R.H., Wang, H.L., Sine, SM., Taylor, P., McCammon, J.A., 2003. Asymmetric structural motions of the homomeric alpha7 nicotinic receptor ligand binding domain revealed by molecular dynamics simulation. Biophys. J. 85, 3007-3018.

Hibbs, R.E., Sulzenbacher, G., Shi, J., Talley, T.T., Conrod, S., Kem, W.R., Taylor, P., Marchot, P., Bourne, Y., 2009. Structural determinants for interaction of partial agonists with acetylcholine binding protein and neuronal alpha7 nicotinic acetylcholine receptor. EMBO J. 28, 3040-3051.

Horenstein, N.A., Papke, R.L., 2017. Anti-inflammatory Silent Agonists. ACS Med. Chem. Lett. 8, 989-991.

Horenstein, N.A,, Papke, R.L., Kulkarni, A.R., Chaturbhuj, G.U., Stokes, C., Manther, K., Thakur. G.A., 2016. Critical molecular determinants of alpha7 nicotinic acetylcholine receptor allosteric activation: separation of direct allosteric activation and positive allosteric modulation. J. Biol. Chem. 291, 5049-5067.

Isaacson, M.D., Horenstein, N.A., Stokes, C., Kem, W.R., Papke, R.L., 2013. Point-to-point ligand-receptor interactions across the subunit interface modulate the induction and stabilization of conformational states of alpha7 nAChR by benzylidene anabaseines. Biochem. Pharmacol. 85, 817-828.

Jordan, C.J., Xi, Z.X., 2018. Discovery and development of varenicline for smoking cessation. Expert Opin Drug Discov. 13, 671-683.

Kabbani, N., Nichols, R.A., 2018. Beyond the Channel: Metabotropic Signaling by Nicotinic Receptors. Trends Pharmacol. Sci. 39, 354-366.

King, J.R., Kabbani, N., 2018. Alpha 7 nicotinic receptors attenuate neurite development through calcium activation of calpain at the growth cone. PLoS One. 13, e0197247.

Kong, F.J., Ma, L.L., Zhang, H.H., Zhou, J.Q., 2015. Alpha 7 nicotinic acetylcholine receptor agonist GTS-21 mitigates isoflurane-induced cognitive impairment in aged rats. J. Surg. Res. 194, 255-261.

Kulkarni, A.R., Thakur, G.A., 2013. Microwave-assisted Expeditious and Efficient Synthesis of Cyclopentene Ring-fused Tetrahydroquinoline Derivatives Using Three-component Povarov Reaction. Tetrahedron Lett. 54, 6592-6595.

Law, R.J., Henchman, R.H., McCammon, J.A., 2005. A gating mechanism proposed from a simulation of a human alpha7 nicotinic acetylcholine receptor. Proc. Natl. Acad. Sci. U S A 102, 6813-6818.

Leiser, S.C., Bowlby, M.R., Comery, T.A., Dunlop, J., 2009. A cog in cognition: how the alpha7 nicotinic acetylcholine receptor is geared towards improving cognitive deficits. Pharmacol. Ther. 122, 302-311.

Li, S.X., Huang, S., Bren, N., Noridomi, K., Dellisanti, C.D., Sine, S.M., Chen, L., 2011. Ligand-binding domain of an alpha7-nicotinic receptor chimera and its complex with agonist. Nat. Neurosci. 14, 1253-1259.

Miller, D.R., Khoshbouei, H., Garai, S., Cantwell, L.N., Stokes, C., Thakur, G., Papke, R.L., 2020. Allosterically Potentiated alpha7 Nicotinic Acetylcholine Receptors: Reduced Calcium Permeability and Current-Independent Control of Intracellular Calcium. Mol. Pharmacol. 98, 695-709.

Nanclares, C., Gameiro-Ros, I., Méndez-López, I., Martínez-Ramírez, C., Padín-Nogueira, J.F., Colmena, I., Baraibar, A.M., Gandía, L., García, A.G., 2018. Dual Antidepressant Duloxetine Blocks Nicotinic Receptor Currents, Calcium Signals and Exocytosis in Chromaffin Cells Stimulated with Acetylcholine. J. Pharmacol. Exp. Ther. 367, 28-39.

Noviello, C.M., Gharpure, A., Mukhtasimova, N., Cabuco, R., Baxter, L., Borek, D., Sine, S.M., Hibbs, R.E., 2021. Structure and gating mechanism of the α_7 nicotinic acetylcholine receptor. Cell. https://doi.org/10.1016/j.cell.2021.02.049.

Papke, R.L., Brunzell, D.H., De Biasi, M., Shoaib, M., Wallace, T.L., 2020a. Cholinergic Receptors and Addiction. Curr. Top. Behav. Neurosci. 45, 123-151.

Papke, R.L., Garai, S., Stokes, C., Horenstein, N.A., Zimmerman, A.D., Abboud, K.A., Thakur, G.A., 2020b. Differing Activity Profiles of the Stereoisomers of 2,3,5,6TMP-TQS, a Putative Silent Allosteric Modulator of alpha7 nAChR. Mol. Pharmacol. 98, 292-302.

Papke, R.L., Stokes, C., Damaj, M.I., Thakur, G.A., Manther, K., Treinin, M., Bagdas, D., Kulkarni, A.R., Horenstein, N.A. 2018a. Persistent activation of alpha7 nicotinic ACh receptors associated with stable induction of different desensitized states. Br. J. Pharmacol. 175, 1838-1854.

Papke, R.L., Peng, C., Kumar, A., Stokes, C., 2018b. NS6740, an alpha7 nicotinic acetylcholine receptor silent agonist, disrupts hippocampal synaptic plasticity. Neurosci. Lett. 677, 6-13.

Papke, R.L., Bagdas, D., Kulkarni, A.R., Gould, T., AlSharari, S., Thakur, G.A., Damaj, M.I., 2015. The analgesic-like properties of the alpha7 nAChR silent agonist NS6740 is associated with nonconducting conformations of the receptor. Neuropharmacology. 91, 34-42.

Papke, R.L., 2014. Merging old and new perspectives on nicotinic acetylcholine receptors. Biochem. Pharmacol. 89, 1-11.

Papke, RL, Horenstein, N.A., Kulkarni, A.R., Stokes, C., Corrie, L.W., Maeng, C.Y., Thakur, G.A., 2014. The activity of GAT107, an allosteric activator and positive modulator of alpha7 nicotinic acetylcholine receptors (nAChR), is regulated by aromatic amino acids that span the subunit interface. J. Biol. Chem. 289, 4515-4531.

Papke, R.L., Trocme-Thibierge C., Guendisch D., Abbas Al Rubaiy S.A., Bloom, S.A., 2011. Electrophysiological perspectives on the therapeutic use of nicotinic acetylcholine receptor partial agonists. J. Pharmacol. Exp. Ther. 337, 367-379.

Papke, R.L., 2010. Tricks of Perspective: Insights and limitations to the study of macroscopic currents for the analysis of nAChR activation and desensitization. J. Mol. Neurosci. 40, 77-86.

Papke, R.L., Stokes, C., 2010. Working with OpusXpress: methods for high volume oocyte experiments. Methods 51, 121-133.

Papke, R.L., Papke, J.K.P., 2002. Comparative pharmacology of rat and human alpha7 nAChR conducted with net charge analysis. Br. J. Pharm. 137, 49-61.

Papke, R.L., Thinschmidt, J.S., 1998. The correction of alpha7 nicotinic acetylcholine receptor concentration-response relationships in *Xenopus* oocytes. Neurosci. Lett. 256, 163-166.

Papke, R.L., Heinemann, S.F., 1994. The partial agonist properties of cytisine on neuronal nicotinic receptors containing the beta2 subunit. Mol. Pharmacol. 45, 142-149.

Peng, C., Kimbrell, M.R., Tian, C., Pack, T.F., Crooks, P.A., Fifer, E.K., Papke, R.L., 2013. Multiple modes of alpha7 nAChR non-competitive antagonism of control agonist-evoked and allosterically enhanced currents. Mol. Pharmacol. 84, 459-475.

Pieschl, R.L., Miller, R., Jones, K.M., Post-Munson, D.J., Chen, P., Newberry, K., Benitex, Y., Molski, T., Morgan, D., McDonald, I.M., Macor, J.E., Olson, R.E., Asaka, Y., Digavalli, S., Easton, A., Herrington, J., Westphal, R.S., Lodge, N.J., Zaczek. R., Bristow, L.J., Li, Y., 2017. Effects of BMS-902483, an alpha7 nicotinic acetylcholine receptor partial agonist, on cognition and sensory gating in relation to receptor occupancy in rodents. Eur. J. Pharmacol. 807, 1-11.

Pismataro, M.C., Horenstein, N.A., Stokes, C., Quadri, M., De Amici, M., Papke, R.L., Dallanoce, C., 2020. Design, synthesis, and electrophysiological evaluation of NS6740 derivatives: Exploration of the structure-activity relationship for alpha7 nicotinic acetylcholine receptor silent activation. Eur. J. Med. Chem. 205, 112669.

Qi, Y., Si, D., Zhu, L., Qi, Y., Wu, Z., Chen, D., Yang, Y., 2020. High-fat diet-induced obesity affects alpha 7 nicotine acetylcholine receptor expressions in mouse lung myeloid cells. Sci. Rep. 10, 18368.

Rosas-Ballina, M., Tracey, K.J., 2009. Cholinergic control of inflammation. J. Intern. Med. 265, 663-679.

Scabia, G., Cancello, R., Dallanoce, C., Berger, S., Matera, C., Dattilo, A., Zulian, A., Barone, I., Ceccarini, G., Santini, F., De Amici, M., Di Blasio, A.M., Maffei. M., 2020. ICH3, a selective alpha7 nicotinic acetylcholine receptor agonist, modulates adipocyte inflammation associated with obesity. J. Endocrinol. Invest. 43, 983-993.

Schaftenaar, G., Noordik, J. H., 2000. Molden: a pre- and post-processing program for molecular and electronic structures. J. Comput. Aid. Mol. Des. 14, 123-134.

Seguela, P., Wadiche, J., Dinely-Miller, K., Dani, J.A., Patrick, J.W., 1993. Molecular cloning, functional properties and distribution of rat brain alpha 7: a nicotinic cation channel highly permeable to calcium. J. Neurosci. 13, 596-604.

Sitzia, F., Brown, J.T., Randall, A.D., Dunlop, J., 2011. Voltage- and Temperature-Dependent Allosteric Modulation of alpha7 Nicotinic Receptors by PNU120596. Front. Pharmacol. 2, 81.

Spurny, R., Debaveye, S., Farinha, A., Veys, K., Vos, A.M., Gossas, T., Atack, J., Bertrand, S., Bertrand, D., Danielson, U.H., Tresadern, G., Ulens, C., 2015. Molecular blueprint of allosteric binding sites in

a homologue of the agonist-binding domain of the alpha7 nicotinic acetylcholine receptor. Proc. Natl. Acad. Sci. U S A 112, E2543-2552.

Stokes, C., Garai, S., Kulkarni, A.R., Cantwell, L.N., Noviello, C.M., Hibbs, R.E., Horenstein, N.A., Abboud, K.A., Thakur, G.A., Papke, R.L., 2019. Heteromeric Neuronal Nicotinic Acetylcholine Receptors with Mutant beta Subunits Acquire Sensitivity to alpha7-Selective Positive Allosteric Modulators. J. Pharmacol. Exp. Ther. 370, 252-268.

Thakur, G.A., Kulkarni, A.R., Deschamps, J.R., Papke, R.L., 2013. Expeditious Synthesis, Enantiomeric Resolution and Enantiomer Functional Characterization of (4-(4-bromophenyl)-3a,4,5,9b-tetrahydro-3H-cyclopenta[c]quinoline-8-sulfonamide (4BP-TQS) an Allosteric agonist –Positive Allosteric Modulator of alpha7 nAChR. J. Med. Chem. 56, 8943-8947.

Thomsen, M.S., Mikkelsen, J.D., 2012. The alpha7 nicotinic acetylcholine receptor ligands methyllycaconitine, NS6740 and GTS-21 reduce lipopolysaccharide-induced TNF-alpha release from microglia. J. Neuroimmunol. 251, 65-72.

Timmermann, D., Sandager-Nielsen, K., Dyhring, T., Smith, M., Jacobsen, A.M., Nielsen, E., Grunnet, M., Christensen, J.K., Peters, D., Kohlhaas, K., Olsen, G.M., Ahring, P.K., 2012. Augmentation of cognitive function by NS9283, a stoichiometry-dependent positive allosteric modulator of alpha2- and alpha4-containing nicotinic acetylcholine receptors. Br. J. Pharmacol. 167, 164-182.

Ulleryd, M.A., Mjörnstedt, F., Panagaki, D., Yang, L.J., Engevall, K., Gutiérrez, S., Wang, Y., Gan, L.M., Nilsson, H., Michaëlsson, E., Johansson, M.E., 2019. Stimulation of alpha 7 nicotinic acetylcholine receptor (α_7nAChR) inhibits atherosclerosis via immunomodulatory effects on myeloid cells. Atherosclerosis 287, 122-133.

Wallace, T.L., Ballard, T.M., Pouzet, B., Riedel, W.J., Wettstein, J.G., 2011. Drug targets for cognitive enhancement in neuropsychiatric disorders. Pharmacol. Biochem. Behav. 99, 130-145.

Walling, D., Marder, S.R., Kane, J., Fleischhacker, W.W., Keefe, R.S., Hosford, D.A., Dvergsten, C., Segreti, A.C., Beaver, J.S., Toler, S.M., Jett, J.E., Dunbar, G.C., 2016. Phase 2 Trial of an Alpha-7

Nicotinic Receptor Agonist (TC-5619) in Negative and Cognitive Symptoms of Schizophrenia. Schizophr. Bull. 42, 335-343.

Wazea, S.A., Wadie, W., Bahgat, A.K., El-Abhar, H.S., 2018. Galantamine anti-colitic effect: Role of alpha-7 nicotinic acetylcholine receptor in modulating Jak/STAT3, NF-κB/HMGB1/RAGE and p-AKT/Bcl-2 pathways. Sci. Rep. 8, 5110.

Williams, D.K., Wang, J., Papke, R.L., 2011a. Positive allosteric modulators as an approach to nicotinic acetylcholine receptor-targeted therapeutics: Advantages and limitations. Biochem. Pharmacol. 82, 915-930.

Williams, D.K., Wang, J., Papke, R.L., 2011b. Investigation of the Molecular Mechanism of the Alpha7 nAChR Positive Allosteric Modulator PNU-120596 Provides Evidence for Two Distinct Desensitized States. Mol. Pharmacol. 80, 1013-1032.

Yang, H., Liu, H., Zeng, Q., Imperato, G.H., Addorisio, M.E,, Li, J., He, M., Cheng, K.F., Al-Abed, Y., Harris, H.E., Chavan, S.S., Andersson, U., Tracey, K.J., 2019. Inhibition of HMGB1/RAGE-mediated endocytosis by HMGB1 antagonist box A, anti-HMGB1 antibodies, and cholinergic agonists suppresses inflammation. Mol. Med. 25, 13.

Zhu, S., Huang, S., Xia, G., Wu, J., Shen, Y., Wang, Y., Ostrom, R.S., Du, A., Shen, C., Xu, C., 2021. Anti-inflammatory effects of α_7-nicotinic ACh receptors are exerted through interactions with adenylyl cyclase-6. Br. J. Pharmacol. 1-15. https://doi.org/10.1111/bph.15412.